Probing Photoelectrochemical Processes in Au−CdS Nanoparticle Arrays by Surface Plasmon Resonance: Application for the Detection of Acetylcholine Esterase Inhibitors

Maya Zayats, Andrei B. Kharitonov, Svetlana P. Pogorelova, Oleg Lioubashevski, Eugenii Katz, and Itamar Willner*

Contribution from the Institute of Chemistry and The Farkas Center for Light-Induced Processes, The Hebrew University of Jerusalem, Jerusalem 91904, Israel

Received August 14, 2003; E-mail: willnea@vms.huji.ac.il

Abstract: The photoelectrochemical charging of Au-nanoparticles (NP) in a Au-nanoparticle/CdS-nanoparticle array assembled on a Au-coated glass surface is followed by means of surface plasmon resonance (SPR) spectroscopy upon continuous irradiation of the sample. The charging of the Au-NPs results in the enhanced coupling between the localized surface plasmon of the Au-NP and the surface plasmon of the bulk surface, leading to a shift in the plasmon angle. The charging effect of the Au-NPs is supported by concomitant electrochemical experiments in the dark. Analysis of the results indicates that ca. 4.2 electrons are associated with each Au-nanoparticle under steady-state irradiation. The photoelectrochemical charging effect of the Au-NPs in the Au−CdS NP array is employed to develop a SPR sensor for acetylcholine esterase inhibitors.

Surface plasmon resonance (SPR) is a versatile method to probe and characterize physicochemical changes of thin films on metal surfaces such as Au or Ag.[1] The assembly of monolayers or thin films on SPR-active surfaces, or chemical transformations occurring on such surfaces, were characterized by SPR spectroscopy. The ability to probe chemical modifiers on surfaces by means of SPR spectroscopy turned the method into a useful analytical tool,[2] and different biorecognition processes, such as protein−protein binding,[3,4] DNA hybridization,[5] or photochemically triggered antigen−antibody association processes,[6] were analyzed by SPR. In most of these systems the chemical modification of the metal surfaces alters the refractive index and thickness of the modified surfaces. Several studies employed Au-nanoparticles (Au-NP) as labels that amplify the SPR signals upon modification of the surfaces. The surface plasmons (SP) are resonantly excited surface electromagnetic waves, which propagate along the planar metal/dielectric interface and are strongly localized in its vicinity.[7] In the presence of the metal-NP layer, part of SP energy, no longer guided by the interface, is transferred outside through scattering within the NP layer. The interactions between the localized surface plasmon (LSP), associated with noble metal NP, and SP on a metal-dielectric interface, that leads to a deformation of the dispersion curve of the SP and to a shift of the plasmon angle, have been observed.[7b] The coupling between the LSP associated with the Au-NP and the surface plasmon wave associated with the interface leads to the enhanced shifts in the plasmon angles upon the chemical modification of the surfaces.[8] Indeed, significant changes in the SPR spectra were reported upon the labeling of antigen−antibody complexes[9] or DNA assemblies[10] with Au-nanoparticles.

Redox transformations occurring on chemically modified surfaces may significantly alter the refractive index of the interface and thus induce change in the plasmon angle of the SPR spectra (angle of minimum reflectance). For example, the

(1) (a) Liebermann, T.; Knoll, W. *Colloids Surf.* **2000**, *171*, 115−130. (b) Knoll, W. *Annu. Rev. Phys. Chem.* **1998**, *49*, 569−638. (c) Frutos, A. G.; Corn, R. M. *Anal. Chem.* **1998**, *A70*, 449A−455A.

(2) (a) Brockman, J. M.; Nelson, B. P.; Corn, R. M. *Annu. Rev. Phys. Chem.* **2000**, *51*, 41−63. (b) Quinn, J. G.; O'Neill, S.; Doyle, A.; McAtamney, C.; Diamond, D.; MacCraith, B. D.; O'Kennedy, R. *Anal. Biochem.* **2000**, *281*, 135−143. (c) Caide, X.; Sui, S.-F. *Sens. Actuators, B* **2000**, *66*, 174−177.

(3) (a) Schuck, P. *Annu. Rev. Biophys. Biomol. Struct.* **1997**, *26*, 541−566. (b) Löfas, S. *Pure Appl. Chem.* **1995**, *67*, 829−834.

(4) (a) Heyse, S.; Ernst, O. P.; Dienes, Z.; Hofmann, K. P.; Vogel, H. *Biochemistry* **1998**, *37*, 507−522. (b) Berger, C. E. H.; Beumer, T. A. M.; Kooyman, R. P. H.; Greve, J. *Anal. Chem.* **1998**, *70*, 703−706. (c) Li, J.; Cook, R.; Doyle, M. L.; Hensley, P.; McNulty, D. E.; Chaiken, I. *Proc. Natl. Acad. Sci. U.S.A.* **1997**, *94*, 6694−6699. (d) Lange, C.; Koch, K.-W. *Biochemistry* **1997**, *36*, 12019−12026.

(5) (a) Peterlinz, K. A.; Georgiadis, R. M.; Herne, T. M.; Tarlov, M. J. *J. Am. Chem. Soc.* **1997**, *119*, 3401−3402. (b) Caruso, F.; Rodda, E.; Furlong, D. N.; Haring, V. *Sens. Actuators, B* **1997**, *41*, 189−197. (c) Bier, F. F.; Kleinjung, F.; Scheller, F. W. *Sens. Actuators, B* **1997**, *38*, 78−82; (d) Thiel, A. J.; Frutos, A. G.; Jordan, C. E.; Corn, R. M.; Smith, L. M. *Anal. Chem.* **1997**, *69*, 4948−4956.

(6) Kaganer, E.; Pogreb, R.; Davidov, D.; Willner, I. *Langmuir* **1999**, *15*, 3920−3923.

(7) (a) Raether, H. *Surface Plasmons*; Springer Tracts in Modern Physics; Vol. 111; Springer-Verlag: Berlin, 1988. (b) Holland, W. R.; Hall, D. G., *Phys. Rev. B* **1983**, *27*, 7765−7768. (c) Kume, T.; Nakagawa, N.; Hayashi, S.; Yamamoto, K. *Solid State Commun.* **1995**, *93*, 171−175.

(8) (a) Lyon, L. A.; Musick, M. D.; Smith, P. C.; Reiss, B. D.; Peña, D. J.; Natan, M. J. *Sens. Actuators B* **1999**, *54*, 118−124. (b) Lyon, L. A.; Peña, D. J.; Natan, M. J. *J. Phys. Chem. B* **1999**, *103*, 5826−5831. (c) Chah, S.; Hutter, E.; Roy, D.; Fendler, J. H.; Yi, J. *Chem. Phys.* **2001**, *272*, 127−136.

(9) Lyon, L. A.; Musick, M. D.; Natan, M. J. *Anal. Chem.* **1998**, *70*, 5177−5183.

(10) He, L.; Musick, M. D.; Nicewarner, S. R.; Sallinas, F. G.; Benkovic, S. J.; Natan, M. J.; Keating, C. D. *J. Am. Chem. Soc.* **2000**, *122*, 9071−9077.

reversible redox processes of polyaniline[11] or Prussian-blue[12] films were transduced by SPR spectroscopy. Furthermore, SPR spectroscopy was employed to follow electrocatalytic[12] and bioelectrocatalytic processes,[13,14] driven by redox-active films associated with gold surfaces. The mediated electron transfer in these systems yields a steady-state ratio between the oxidized and reduced forms of the interface, resulting in SPR spectra that exhibit intermediary patterns of the two interface states. This enabled the development of SPR-based electrochemical sensors.

The photochemical functionalities of semiconductor nanoparticles associated with electrodes were a subject of extensive research efforts in the past decade.[15,16] Within these scientific efforts, the understanding of the photophysical properties of metal−semiconductor (e.g., Au−TiO$_2$) nanoclusters is of particular interest.[17] It was demonstrated that electron-transfer of conduction-band electrons from the semiconductor to the metal nanoclusters enhances the charge separation and thus decreases the electron−hole pairs recombination. This observation was further developed by the tailoring of organized layered assemblies of Au-NP and CdS-NP on electrode surfaces for enhanced photocurrent generation.[18] Photoinduced electron transfer from CdS-NP to the Au-NP results in the separation of the electron−hole pairs in the two different particle entities against recombination. The subsequent transfer of the Au-NP-captured electrons to the electrode leads to the enhanced photocurrent in the system. Thus, one may anticipate that upon the photochemical excitation of the Au−CdS nanoparticle system, the Au-NP will be charged by electrons, and the charge density will be controlled by the effectiveness of the photoinduced charge separation in the system. It is known that addition or removal of some number of electrons from noble metal NP produces a notable shift in LSP band position, and efforts have been made to account for such LSP band shifts using Mie theory.[19] These spectral shifts of nanoparticle LSP band position in aqueous solution as well as on the electrode surface are attributed to the changes in plasma frequency, caused by the charge density increase resulting from the charging of Au-NP core.[19b,c] For example, causing the Au-NP core to be electron-deficient by changing the potential from −0.16 to +0.82 V (versus Ag quasi-reference electrode) causes the LSP band to move to lower energy.[19c] Since the localized plasmon of Au-NP immobilized on the interface is coupled to the bulk gold surface plasmon, the charging of the particles would alter not only LSP band position but also the coupling between the Au-NP and the surface plasmon wave, resulting in the change in the SPR spectrum. Also, the charging of the Au-NP array is anticipated to change the potential distribution across the electrode interface.

Here we wish to report on the probing of photoelectrochemical properties of the Au−CdS nanoparticles array by means of SPR spectroscopy. Observed plasmon angle shifts and photovoltage generated on the electrode were interpreted as originating from photoinduced charge injection into the outermost layer of the Au-NP.

As far as we are aware, this is the first example demonstrating the combination of SPR spectroscopy with photoelectrochemical charging of Au-NP. Furthermore, recently enzyme-functionalized CdS nanoparticle hybrids associated with electrodes were used as photoelectrochemical biosensors.[20] For example, acetylcholine esterase-functionalized CdS nanoparticles on electrodes were employed as active interfaces for photocurrent generation and for the electrochemical transduction of the biocatalyst inhibition. In the present study we demonstrate the SPR read-out of the inhibition of acetylcholine esterase upon the irradiation of an interface consisting of the biocatalyst and a layered Au−CdS nanoparticle assembly.

Experimental Section

Chemicals. Acetylcholine esterase (AChE, EC 3.1.1.7, type VI-S from electric eel), acetylthiocholine, 1,5-bis(4-allyldimethylammoniumphenyl)pentane-3-one dibromide (anticholinesterase BW284c51) were purchased from Sigma and used without further purification. All other chemicals, including 2,2′-dithio-bis(ethaneamine) (cystamine), 4-(2-hydroxyethyl)-piperazine-1-ethanesulfonic acid sodium salt (HEPES), 1-[3-(dimethylamino)-propyl]-3-ethylcarbodiimide hydrochloride (EDC), glutaric dialdehyde, sodium bis(2-ethylhexyl)sulfosuccinate (AOT), cadmium perchlorate hydrate, sodium sulfide, 2-aminoethanethiol (cysteamine), 2-mercaptoethanesulfonic acid, *N*-2-mercaptopropionylglycine (tiopronin), HAuCl$_4$·3H$_2$O (99,999%), sodium borohydride (98%), triethanolamine hydrochloride (TEA) were purchased from Sigma and Aldrich and used as supplied. Ultrapure water from Barnstead NANOpure Diamond system was used in all experiments. The CdS-nanoparticles (CdS-NP) were prepared in AOT/heptane reverse micelles.[21] The surfaces of the resulting CdS-NP were modified both with 2-aminoethanethiol and with 2-mercaptoethanesulfonic acid as described in the literature.[22] The tiopronin-functionalized gold nanoparticles were prepared as described in the literature.[23]

Modification of Electrodes. Glass supports (20 mm × 20 mm) covered with a chromium sublayer (∼5 nm) and a gold layer (∼50 nm) (Analytical-μSystem, Germany) were used for the SPR measurements and as working electrodes (with 0.38 cm^2 area exposed to the solution and to irradiation). Prior to the modification the surfaces of

(11) (a) Chegel, V.; Raitman, O. A.; Katz, E.; Gabai, R.; Willner, I. *Chem. Commun.* **2001**, *10*, 883−884. (b) Baba, A.; Park, M.-K.; Advincula, R. C.; Knoll, W. *Langmuir* **2002**, *18*, 4648−4652. (c) Baba, A.; Advincula, R. C.; Knoll, W. *J. Phys. Chem. B* **2002**, *106*, 1581−1587.

(12) Raitman, O. A.; Katz, E.; Willner, I.; Chegel, V. I.; Popova, G. V. *Angew. Chem., Int. Ed.* **2001**, *40*, 3649−3652.

(13) Raitman, O. A.; Katz, E.; Bückmann, A. F.; Willner, I. *J. Am. Chem. Soc.* **2002**, *124*, 6487−6496.

(14) Raitman, O. A.; Patolsky, F.; Katz, E.; Willner, I. *Chem. Commun.* **2002**, 1936−1937.

(15) (a) Klein, D. L.; Roth, R.; Lim, A. K. L.; Alivisatos, A. P.; McEuen, P. L. *Nature* **1997**, *389*, 699−701. (b) Alivisatos, A. P. *Science* **1996**, *271*, 933−937. (c) Kim, T. W.; Lee, D. U.; Yoon, Y. S. *J. Appl. Phys.* **2000**, *88*, 3759−3761. (d) Niemeyer, C. M. *Angew. Chem., Int. Ed.* **2001**, *40*, 4128−4158.

(16) (a) Bruchez, M., Jr.; Moronne, M.; Gin, P.; Weiss, S.; Alivisatos, A. P. *Science* **1998**, *281*, 2013−2015. (b) Chan, W. C. W.; Nie, S. *Science* **1998**, *281*, 2016−2018. (c) Tessler, N.; Medvedev, V.; Kazes, M.; Kan, S.; Banin, U. *Science* **2002**, *295*, 1506−1508. (d) Pavesi, L.; Negro, L. D.; Mazzoleni, C.; Franzo, G.; Priolo, F. *Nature* **2000**, *408*, 440−444. (e) Malko, A. V.; Mikhailovsky, A. A.; Petruska, M. A.; Hollingsworth, J. A.; Htoon, H.; Bawendi, M. G.; Klimov, V. I. *Appl. Phys. Lett.* **2002**, *81*, 1303−1305.

(17) (a) Chandrasekharan, N.; Kamat, P. V. *J. Phys. Chem. B* **2000**, *104*, 10851−10857. (b) Subramanian, V.; Wolf, E.; Kamat, P. V. *J. Phys. Chem. B* **2001**, *105*, 11439−11446. (c) Subramanian, V.; Wolf, E. E.; Kamat, P. V. *Langmuir* **2003**, *19*, 469−474.

(18) Sheeney-Haj-Ichia, L.; Pogorelova, S. P.; Willner, I. *Adv. Funct. Mater.* **2003**. In press.

(19) (a) Henglein, A.; Mulvaney, P.; Linnert, T. *Discuss. Faraday Soc.* **1991**, *92*, 33. (b) Ung, T.; Giersig, M.; Dunstan, D.; Mulvaney, P. *Langmuir* **1997**, *13*, 1773−1782. (c) Templeton, A. C.; Pietron, J. J.; Murray, R. W.; Mulvaney, P. *J. Phys. Chem. B* **2000**, *104*, 564−570.

(20) Pardo-Yissar, V.; Katz, E.; Wasserman, J.; Willner, I. *J. Am. Chem. Soc.* **2003**, *125*, 622−623.

(21) (a) Steigerwald, M. L.; Alivisatos, A. P.; Gibson, J. M.; Harris, T. D.; Kortan, R.; Muller, A. J.; Thayer, A. M.; Duncan, T. M.; Douglass, D. C.; Brus, L. E. *J. Am. Chem. Soc.* **1988**, *110*, 3046−3050. (b) Kortan, A. R.; Hull, R.; Opila, R. L.; Bawendi, M. G.; Steigerwald, M. L.; Carrol, P. J.; Brus, L. E. *J. Am. Chem. Soc.* **1990**, *112*, 1327−1332.

(22) Miyake, M.; Matsumoto, H.; Nishizawa, M.; Sakata, T.; Mori, H.; Kuwabata, S.; Yoneyama, H. *Langmuir* **1997**, *13*, 742−746.

(23) Templeton, A. C.; Chen, S.; Gross, S. H.; Murray, R. W. *Langmuir* **1999**, *15*, 66−76.

Au-electrodes were cleaned with hot ethanol followed by rinsing with water, after which the electrodes were soaked in an aqueous 50 mM cystamine solution for 2 h and then rinsed thoroughly with water to remove any physically adsorbed cystamine. The cystamine-modified electrodes were incubated for 2 h in a solution of the tiopronin-capped Au-NP (1 mg·mL^{-1}) in 0.1 M HEPES buffer, pH = 7.2, in the presence of 5 mM EDC. The Au-NP-functionalized electrodes were then reacted with the cysteamine-stabilized CdS-NP (1 mg·mL^{-1}) solution in 0.1 M HEPES buffer, pH = 7.2, in the presence of 5 mM EDC for 2 h. The electrodes were then rinsed with water to remove the physically adsorbed material. For further functionalization with the enzyme, acetylcholine esterase (AchE), the electrodes were activated with glutaric dialdehyde by dipping the electrodes in a solution of glutaric dialdehyde 10% (v/v) in 0.1 M phosphate buffer, pH = 7.0, for 20 min. After that, the electrodes were briefly washed with water, and then reacted with AChE (1 mg·mL^{-1}) in 0.1 M phosphate buffer, pH = 7.0, for 20 min at room temperature. The resulting Au-electrodes were washed with water to yield the Au-NP/CdS-NP/AChE hybrid array. For control experiments the electrodes were functionalized with cysteamine-stabilized CdS-NP, omitting the modified Au-NP. The cystamine-modified Au-electrodes were reacted with glutaric dialdehyde, 10% (v/v) in 0.1 M phosphate buffer, pH = 7.0, for 20 min. After that, the electrodes were rinsed with water, and then reacted with CdS-NP (1 mg·mL^{-1}) in 0.1 M phosphate buffer, pH = 7.0, for 20 min at room temperature. The electrodes functionalized with CdS-NP were rinsed with water to remove any physically adsorbed materials.

In Situ Photoelectrochemical-SPR Measurements. The surface plasmon resonance (SPR) Kretschmann type spectrometer Biosuplar-2 (Analytical-μSystem, Germany) with a light-emitting diode light source, $\lambda = 670$ nm, prism refraction index $n = 1.61$, and a dynamic angle range up to 19° in air was used in this work. The SPR data were processed using Biosuplar-2 software (version 2.2.30). The SPR sensograms (time-dependent changes of the reflectance minimum) represent real-time changes in the plasmon angle, and these were recorded using a home-built open cell under the flow of Ar. An auxiliary Pt and a quasi-reference Ag electrode inserted into the cell were made from wires of 0.5-mm diameter. Multipotential step chronoamperometry experiments were performed using an electrochemical analyzer (EG&G, VersaStat) linked to a computer (EG&G Software no.270/250). The measured potentials are reported versus Ag-quasi-reference electrode. The SPR sensograms were measured in situ upon application of an external potential onto the working electrode.

A blue light-emitting diode (LED UB 5306X with peak emission at $\lambda = 460$ nm, spectrum half-width 30 nm) was employed as a light source for the irradiation. The measured light power (at forward current 20 mA) was about 1.5 mW, and this corresponds to a photon flux ca. 3.4×10^{18} photons sec^{-1}. For the photovoltage measurements a Keithley electrometer (model 617, input impedance greater than 40 TΩ) has been used. The size distributions of Au-NP and CdS-NP were determined by a Technai-12 FEI Philips transmission electron microscope (TEM) operated at 120 kV. Samples used for the TEM observations were prepared by placing a droplet of the nanoparticles dissolved in water onto a Cu grid with amorphous carbon overlayers followed by drying under vacuum.

For the photocurrent measurements we used a home-built photo-electrochemical system that consists of a Xe lamp (Oriel, model 6258, 300 W), a monochromator (Oriel, model 74000), and a chopper (Oriel, model 76994). The electrical output from the cell was sampled by a lock-in amplifier (Stanford Research, model SR 830 DSP). The shutter chopping frequency was controlled by a pulse/delay generator (Stanford Research, model DE 535). The photogenerated current was measured between the working electrode and the counter electrode (graphite electrode). The photoelectrochemical measurements were performed in 0.1 M phosphate buffer, pH = 10, in the presence of various concentrations of TEA under Ar at ambient temperature (23 ± 2 C°).

Microgravimetric Measurements. A QCM analyzer (Fluke 164T multifunction counter, 1.3 GHz, TCXO) linked to a computer with the homemade software was used for microgravimetric measurements. Quartz crystals (AT-cut, ca. 9 MHz, EG&G) sandwiched between two Au electrodes (geometrical area 0.2 cm^2, roughness factor ca. 3.5) were used. The Au electrode surfaces were washed with ethanol and modified in the same way as that described for Au-coated glass slides. Frequency changes of the quartz crystals were measured in air after each modification step. All the measurements were carried out at ambient temperature (23 ± 2 °C).

Impedance Spectroscopy Measurements. Non-Faradaic impedance measurements were performed in the frequency range of 100 mHz to 10 kHz in 0.1 M phosphate buffer, pH = 7, under Ar, using the electrochemical analyzer (model 6310, EG&G) connected to a personal computer (EG&G software 398). The tiopronin-modified electrode was biased in the potential range of 0.3 to −0.3 V. The experimental impedance spectra were fitted to the equivalent circuit consisting of the resistance and the constant phase element connected in series using commercial software (Zview, version 2.1b, Scribner Associates Inc.).
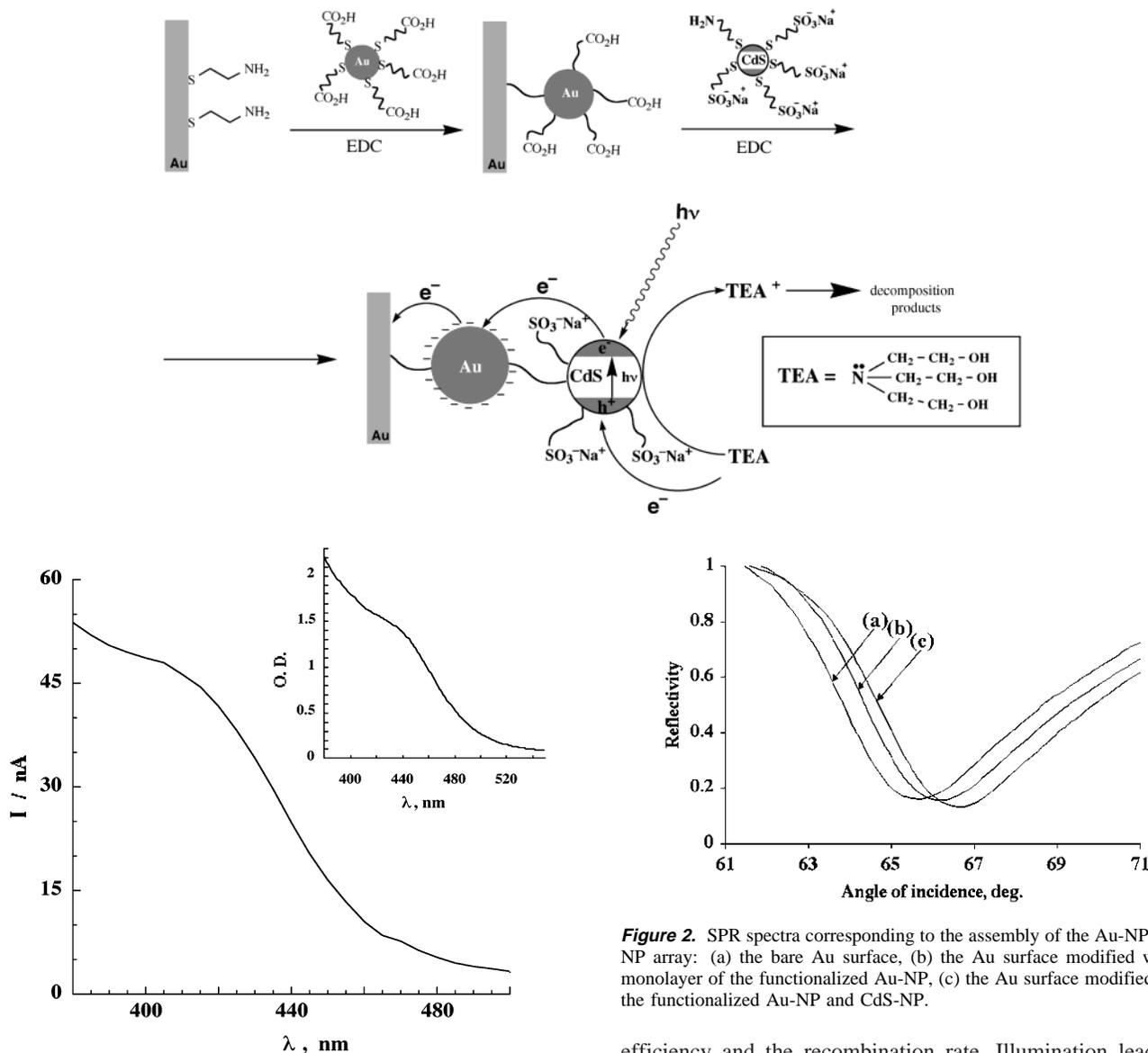
Results and Discussion

According to the TEM measurements the mean sizes of the NPs' cores were estimated to be 2.3 ± 0.5 nm and 5 ± 1.1 nm for the Au-NPs and for the CdS-NPs, respectively. Scheme 1 depicts the method to assemble the Au- and CdS-nanoparticle arrays on the gold-coated glass slides. The tiopronin-modified Au-NPs were covalently linked to a cystamine monolayer associated with the Au-surface. Then the CdS-NPs stabilized with a mixed monolayer consisting of cysteamine and of 2-mercaptoethanesulfonic acid were covalently linked to the Au-nanoparticle layer. The assembly of the Au-NP/CdS-NP array on Au-quartz QCM electrodes indicates that the surface coverage of the Au-NP and of the CdS-NP corresponds to ca. 3.8×10^{-11} mol·cm^{-2} and 2.0×10^{-12} mol·cm^{-2}, respectively. These measurements suggest that the deposition coverage of Au-NP yields ca. 95% of a 2D densely packed NP monolayer, while for the CdS-NP the surface coverage is only ca. 10% of a densely packed NP monolayer. Using values of the surface coverage we conclude that each CdS-NP is linked to ca. 5 of the Au-NPs and that ca. 50% of the Au-NPs are in contact with the CdS-NPs.

The photocurrent action spectrum of the system shown in Scheme 1 is depicted in Figure 1. The photocurrent spectrum generated upon irradiation of the nanoparticle system overlaps the absorption spectrum of the CdS-NP (Figure 1, inset), indicating that the photocurrent originates from the excitation of the semiconductor nanoparticles, resulting in the electron−hole formation. The scavenging of the valence-band holes by electron donor, TEA, results in accumulation of electrons in the conduction band and their transport to the electrode. This background experiment reveals the photoelectrochemical activities of the Au-NP/CdS-NP system.

In contrast to the previous experiment that was performed under short-circuit conditions, in the rest of the present work we studied the Au−CdS nanoparticle arrays in the open-circuit configuration under continuous irradiation. Figure 2 shows the SPR spectra observed upon the build-up of the Au−CdS nanoparticle arrays on the Au-coated glass slides. Clearly, the association of the Au-NP to the interface shifts significantly the plasmon angle due to the plasmon coupling between the LSP of the nanoparticle and the SP of the bulk electrode. The binding of covalently linked CdS nanoparticles further shifts

Scheme 1. Stepwise Assembly of the Photoelectrochemical System Composed of Functionalized Au and CdS Nanoparticles on a Au Electrode Surface and Its Operation upon Illumination
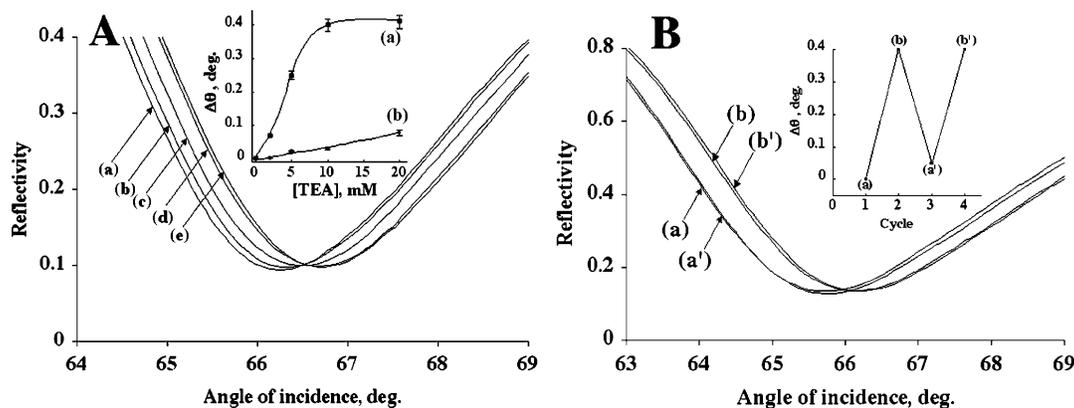

Figure 1. Photocurrent action spectrum generated upon the irradiation under Ar of the array shown in Scheme 1. Electrolyte solution consisted of 0.1 M phosphate buffer, pH = 10, that included TEA, 20 mM. Inset: Absorption spectrum of CdS-NP.

Figure 2. SPR spectra corresponding to the assembly of the Au-NP/CdS-NP array: (a) the bare Au surface, (b) the Au surface modified with a monolayer of the functionalized Au-NP, (c) the Au surface modified with the functionalized Au-NP and CdS-NP.

the plasmon angle due to enhanced SP scattering and possible changes of the refractive index of the interface. Figure 3A shows the SPR spectra observed upon the irradiation of the Au-NP/CdS-NP array in the presence of different concentrations of the sacrificial electron donor, TEA. Irradiation of the Au−CdS array in the absence of TEA does not alter the SPR spectrum, curve (a), as compared to the spectrum recorded in the dark. As the concentration of TEA increases, the plasmon angle of the SPR spectra is shifted to higher values, curves (b−e), and the change in the plasmon angle reaches a saturated shift that corresponds to $\Delta\theta = 0.4°$ at TEA concentrations higher than 1×10^{-2} M, Figure 3A, inset, curve (a). The changes in the plasmon angles, Figure 3A, inset, curve (a), are calculated relative to the plasmon angles of the systems including similar TEA concentrations in the dark. The number of electrons accumulated in the conduction band is defined by the competition between the excitation

efficiency and the recombination rate. Illumination leads to electron accumulation in the conduction band, and the CdS-NP quasi Fermi level moves up toward the low edge of the conduction band energy level. Thus, since the concentration of TEA at a given efficiency of charge separation defines the electron−hole recombination rate, it should define the value of the quasi-Fermi level of CdS-NP, depending on the concentration of electrons in the conduction band. Upon the electron transfer to the Au-NP, the Fermi level of the Au-NP is shifted negatively until it merges with the CdS-NP conduction band low edge. We believe that the saturation of the plasmon angle shift is caused by the equilibration of the Fermi levels of Au-NP and the low edge of the CdS-NP conduction band, following the electron transfer from CdS-NP to the Au-NP. Recently the process of Fermi level equilibration in ZnO quantum dot−metal nanojunctions has been observed by using changes of the surface plasmon band of the metal nano-islands following the photo-induced electron accumulation.[24]

(24) Wood, A.; Giersig, M.; Mulvaney P. *J. Phys. Chem. B* **2001**, *105*, 8810−8815.
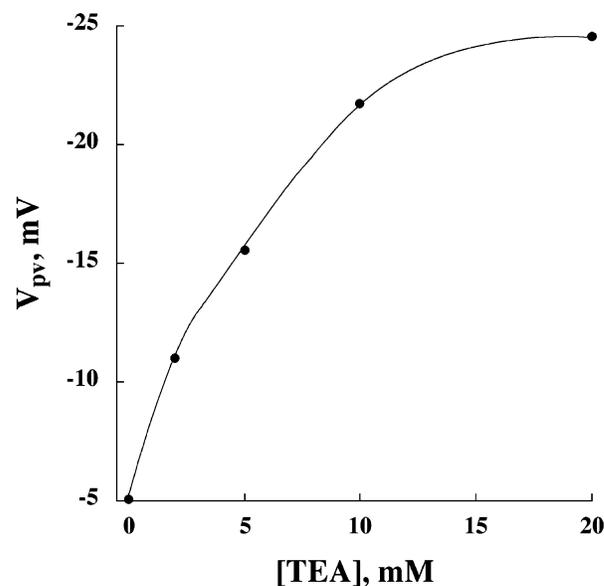
Figure 3. (A) SPR spectra of the Au surface modified with Au-NP/CdS-NP array upon illumination in the presence of various concentrations of TEA: (a) 0 mM, (b) 2 mM, (c) 5 mM, (d) 10 mM, (e) 20 mM. Inset: The plasmon angle shifts upon: (a) The irradiation of the Au electrode modified with Au-NP/CdS-NP array in the presence of different concentrations of TEA. (b) The irradiation of the Au electrode modified with a monolayer of the CdS-NP in the presence of different concentrations of TEA. (B) The SPR spectra of the Au surface modified with the functionalized Au-NP/CdS-NP array: (a–a′) dark, (b–b′) under irradiation. Inset: Reversible shifts of the plasmon angle upon irradiation and dark conditions.

Figure 3A, inset, curve (b), shows the changes in the plasmon angles upon the irradiation of the CdS-nanoparticle array linked to the electrode in the absence of the intermediary Au-NP. The shift in the plasmon angle corresponds to ca. 0.1°, and this is explained by charge transfer to the surface states of CdS-NP. Indeed a charge-induced absorption-edge shift has been observed earlier for thin CdS layers.[25] These results clearly indicate that the SPR spectrum of the Au−CdS nanoparticle array is strongly affected by the irradiation of the system in open circuit configuration. These effects are rationalized in terms of the electron transfer from the CdS-NP to the Au-NP and the sequential charge storage on the Au-NP.

The effect of light on the SPR spectra of the Au−CdS nanoparticle array is reversible, and upon the cyclic switching "ON" and "OFF" of the external light source, the plasmon angle is switched between high and low values, Figure 3B and inset. Thus, the plasmon angle may be used as the transduction means of the optical signal that activates the charging of Au-NP array. It should be noted that the nanoparticle-functionalized Au surfaces reveal stability, and upon repeated washing (four cycles) the results could be reproduced within 5%.

Additional experiments were performed to elucidate the charging that occurs in the irradiated Au−CdS nanoparticle array with the attempt to correlate these changes with the resulting plasmon angle shift. The surface photovoltage, V_{PV}, is defined as the illumination-induced change in the surface potential, ($V_{PV} = V_{light} − V_{dark}$). The photovoltaic effect is the result of charge transfer and/or redistribution within the system due to the irradiation. Since the electric potential and the charge distribution are interdependent through the Poisson and continuity equations, the stored charge, and hence the surface potential, changes upon irradiation. It is important to note that the formation of V_{PV} occurs only if charge generation per se is followed by net spatial charge redistribution. Figure 4 shows the photovoltage, V_{PV}, generated on the electrode that includes the Au−CdS nanoparticle array upon irradiation of the system under open-circuit conditions in the presence of different concentrations of the sacrificial electron donor, TEA. The photovoltage increases as the concentration of TEA is elevated, and it reaches a saturation value of $V_{PV} = −25$ mV at TEA concentrations of $1 \times 10^{−2}$ M

(25) Liu, C. Y.; Bard, A. J. _J. Phys. Chem._ **1989**, _93_, 7749−50.
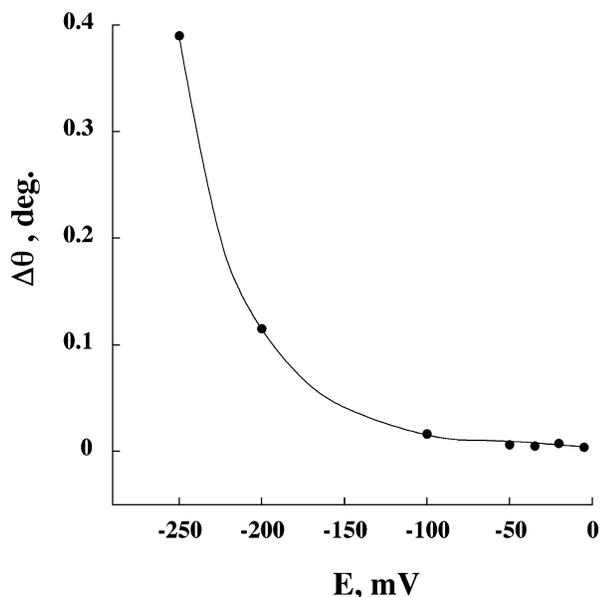
Figure 4. Photovoltage measured on the Au electrode modified with the Au-NP/CdS-NP array upon its illumination in the presence of various concentrations of TEA.

and higher. At these concentrations of TEA the plasmon angle of the SPR spectrum is shifted by $\Delta\theta = 0.4°$ as compared to the nonilluminated Au−CdS nanoparticle array. Thus, at the conditions where the irradiation of the system leads to the maximum changes in the plasmon angle of the SPR spectrum, the photovoltage on the gold electrode is −25 mV. In a control experiment the Au-NP array was irradiated in the presence of TEA, $2 \times 10^{−2}$ M (no CdS-NP array). A minute shift in V_{PV}, ca. 5 mV, was observed that could originate from the minor photochemical activity of the Ag-quasi-reference electrode.

Provided that the charging of the Au-NP core leads to the observed changes in the plasmon angle, that are accompanied by changes in V_{PV}, one may perform the reverse dark experiment where a negative potential is applied on the same electrode that contains the Au−CdS nanoparticle array. Figure 5 shows the changes in the plasmon angle of the Au−CdS nanoparticle system at different applied potentials in the dark. At an applied potential of −225 mV on the bulk electrode, the change in the plasmon angle ($\Delta\theta = 0.4°$) is similar to that observed under

Figure 5. The plasmon angle shift observed at the Au electrode modified with the Au-NP/CdS-NP array upon application of variable potentials to the electrode in the dark in the presence of TEA, 20 mM.

irradiation, resulted in a photovoltage, V_{PV}, of -25 mV on the Au-electrode. As the changes in the plasmon angle of the cystamine-coated Au-electrode upon application of the same potential of -225 mV are minute (ca. 0.05 °), the observed changes in the plasmon angle of the sample containing nano-particles array originate from the charging of the Au-NP as a result of the application of the negative potential on the macroscopic Au-electrode. Charging of the Au-NP alters the coupling between the LSP of the particle and the SP of the bulk gold, and this leads to the changes in the plasmon angle.

While upon irradiation of the Au−CdS nanoparticle array the value of photopotential generated on the bulk electrode is -25 mV, an external potential of -225 mV has to be applied on the bulk electrode to gain a similar change in the plasmon angle of the system in the dark (or to obtain the similar charging of the Au-NP obtained under irradiation). Thus, one may conclude that a resistance for the electron transfer (tunneling) between the tiopronin-capped Au-NP and the bulk electrode results in a potential drop across the tiopronin−cystamine layer. It is well-known that a molecular monolayer provides both the supporting layer and the tunneling barrier for the electron transfer across them, originating from the high resistance of the layer.[26] Since this resistance for the electron transfer causes the potential drop, V_{th}, it is necessary to apply a high negative external potential on the electrode to reach the respective potential on the Au-NP. Assuming an equal potential drop for any direction of the potential, applied to the cystamine−tiopronin layer, we can calculate the potential on the Au-NP, V_D, generated either by the light-induced process or by the applied potential in the dark, that yields the same plasmon angle shift of 0.4°. The Au-NP potential under steady-state irradia-tion, V_D, may be expressed by eq 1

$$V_D = V_{th} + V_{PV} \qquad (1)$$

(26) Finklea, H. O. In *Electroanalytical chemistry*; Bard, A. J., Rubinstein, I., Eds.; Marcel Dekker: New York, 1996; Vol. 19, pp 110−318.

where V_{th} is the potential drop across the cystamine−tiopronin layer, and V_{PV} is the photopotential measured at electrode. The obtained value of V_D is found to be -125 mV, and hence V_{th} is equal to -100 mV.

We conclude that the large changes in the plasmon angles of the illuminated Au−CdS nanoparticle array probably originate from the photoinduced charging of the Au-NP. The higher electron density in the nanoparticle alters the LP frequency,[27] and hence the coupling of the particle LP with the surface plasmon of the gold interface, that should result in a shift in the plasmon angle. It should be noted that this potential drop across the monolayer suggests a high local electric field in the order of magnitude of 10^8 V/cm. This value is consistent with the value of local electric field across monolayer assemblies that were extracted from $I-V$ curves of related systems (10^7-10^9 V/cm).[28]
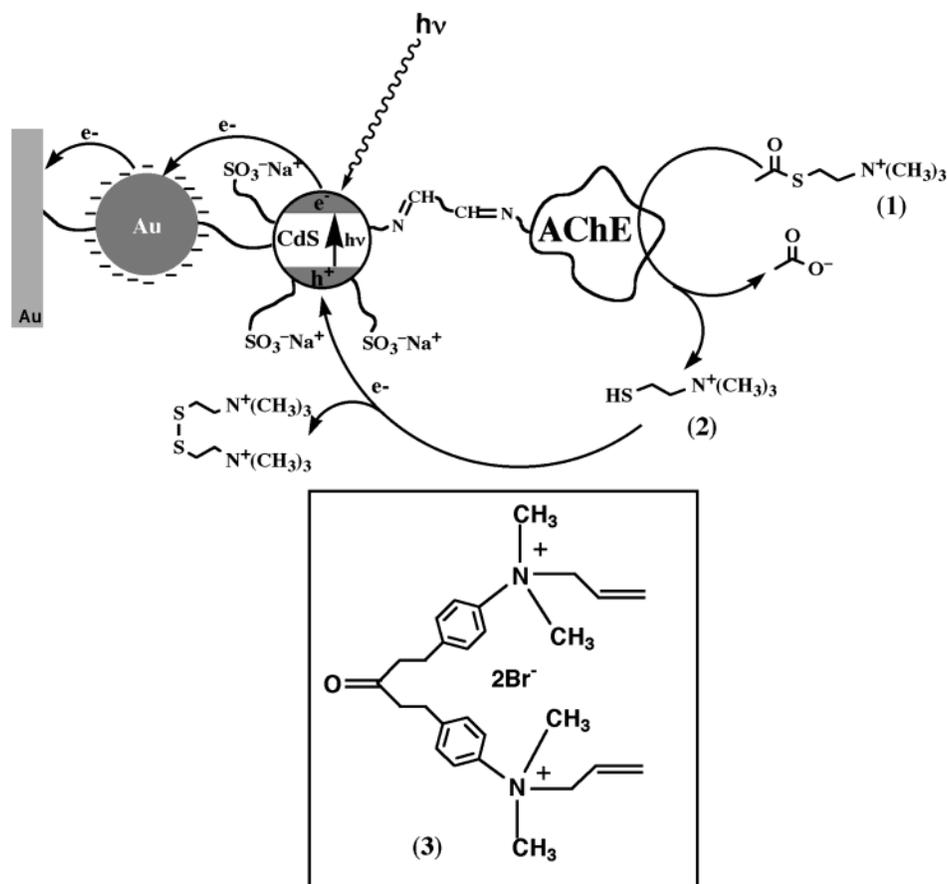
For the better understanding of the mechanism leading to the photochemical charging of the Au-NP we made an effort to estimate quantitatively the degree of Au-NP charging. An ionic space charge layer is formed around the Au-NP core, and it is separated from the core by the capping monolayer that serves as a dielectric medium of the double-layer capacitor. In the studies of Murray and co-workers[29] it was reported that the double-layer capacitance of monolayer-protected Au-NP in an electrolyte solution is well described by the simple concentric sphere model, eq 2

$$C_{AuNP} = 4\pi\epsilon\epsilon_0 r(r + d)/d \qquad (2)$$

where C_{AuNP} is the capacitance of an individual Au-NP, r is the metal core radius, ϵ and d are the static dielectric constant and the thickness of the capping monolayer, respectively. We apply this model to the Au-NPs studied by us that exhibit a core diameter of 2.3 nm and the tiopronin monolayer of a thickness of 0.7 nm, as a capping interface. Using the extracted value for the dielectric constant[30−32] of the tiopronin layer of ca. 16, we obtained a capacitance value of $C_{AuNP} = 5.4$ aF for a single Au-NP. Thus, a storage of a single electron on the Au-

(27) Ashcroft, N. W.; Mermin, N. D. *Solid State Physics*; Holt, Rinehart & Winston: New York, 1976.
(28) Adams, D. M.; Brus, L.; Chidsey, C. E. D.; Creager, S.; Creutz, C.; Kagan, C. R.; Kamat, P. V.; Lieberman, M.; Lindsay, S.; Marcus, R. A.; Metzger, R. M.; Michel-Beyerle, M. E.; Miller, J. R.; Newton, M. D.; Rolison, D. R.; Sankey, O.; Schanze, K. S.; Yardley, J.; Zhu, X. Y. *J. Phys. Chem. B* **2003**, *107*, 6668−6697.
(29) Hicks, J. F.; Templeton, A. C.; Chen, S.; Schaaf, T. G.; Whetten, R. L.; Murray, R. W. *Anal. Chem.* **1999**, *71*, 3703−3711.
(30) The interfacial capacitance of the bulk Au-electrode modified by the tiopronin monolayer was obtained from impedance spectroscopy measure-ments, and the data were fitted to the equivalent circuit composed of a resistance and a constant phase element (CPE) in series. The impedance of a CPE is given by $Z_{CPE}(\omega) = C^{-1}(j\omega)^{-n}$. For an ideal capacitor, n will be equal to 1.[31] For the tiopronin-modified electrode the value for n was found to be ca. 0.96; thus, the CPE was considered as mainly capacitance. The minimum value of the interfacial capacitance, corresponding to the zero-charge potential ($E_{ZCP} = -0.1$ V) was found to be ca. 14 μF cm^{-2}. Assuming that the interfacial capacitance consists of a bare gold electrode capacitance (measured value ca. 52 μF cm^{-2}) and the capacitance of the tiopronin monolayer connected in series, the later was found to be ca. 20 μF cm^{-2}. The static dielectric constant of the tiopronin monolayer was calculated using the formula for the ideal flat capacitor, and the obtained value[31] of ϵ equals to ca. 16. This result implies that the specific capacitance of the tiopronin monolayer is higher than the analogous specific capacitance of the 2D-SAM monolayers formed on Au surfaces with alkanethiolates,[26] because of the higher dielectric constant of the tiopronin.
(31) Macdonalds, J. R., Ed. *Impedance Spectroscopy*; Wiley-Interscience: New York, 1987.
(32) The derived dielectric constant reveals an apparent low value as compared to polar molecules of similar structure. This is explained by the fact that tiopronin is bound to the electrode surface and its mobility is hindered by the charged double layer.[33]

Scheme 2. Photobioelectrochemical System Composed of the Au-NP/CdS−NP/Acetylcholine Esterase Hybrid and Its Operation under Illumination in the Presence of Acetylthiocholine

NP of that capacitance will change its potential by a step corresponding to $\Delta V = e/C_{AuNP} = 30$ mV, where e is the charge of electron (1.602×10^{-19} C).

To extract the average number of electrons that are accumulated on an individual nanoparticle, one has to calculate the potential generated on a single nanoparticle and translate it to the number of electrons per particle using the calculated capacitance, C_{AuNP}. The potential V_D is generated by the charge Q, accumulated on the Au-NP that is proportional to the number of stored electrons in the particle, N, accumulated under steady-state irradiation, where $Q = Ne$. Assuming that the Au-NP layer is an equipotential layer, the Au-nanoparticle potential, V_D, may be expressed by eq 3
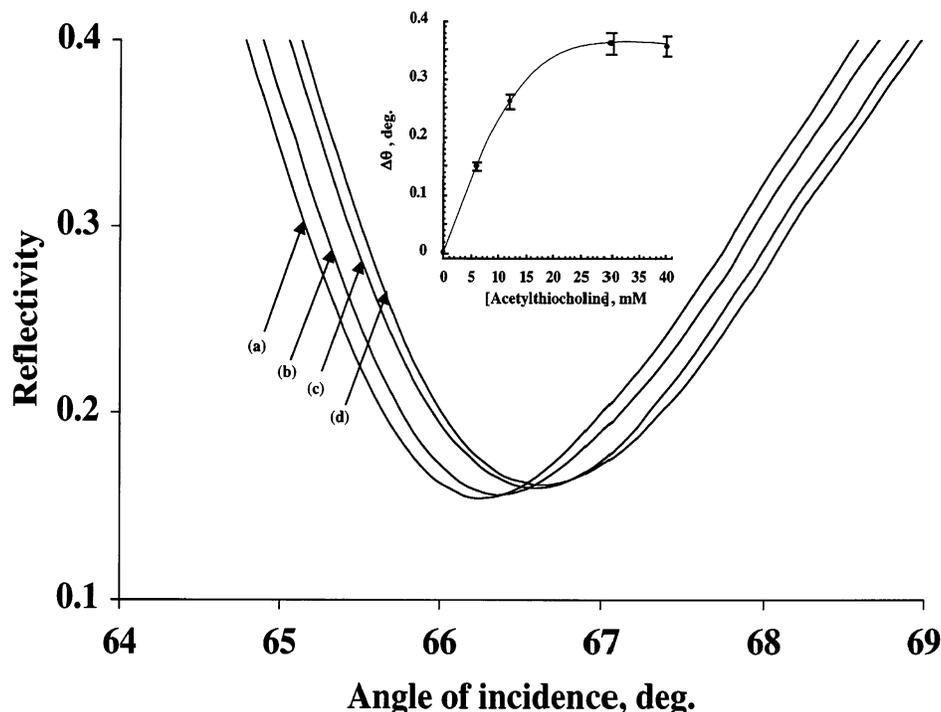
$$V_D = Ne/C_{AuNP} \qquad (3)$$

where C_{AuNP} is the capacitance of the double-layer of monolayer-protected Au-NP. Dividing the extracted V_D value (-125 mV) by the calculated value of ΔV (30 mV) we estimate that ca. 4.2 electrons are associated with each Au-NP under steady-state irradiation. Thus, the use of the SPR spectroscopy upon irradiation together with the concomitant voltage measurements in the dark revealed the mean number of electrons stored on Au-NP.

The enzyme−Au/CdS nanoparticle system may be employed as a versatile photoelectrochemical label for biosensing events. Acetylcholine is a central neurotransmitter that activates the synapse and the neural response. After activating the neural system, it is rapidly hydrolyzed by the serine protease acetyl-

holine esterase (AChE) to restore the resting potential of the synaptic membrane. Different reagents, such as the nerve gas diisopropyl fluorophosphate (Sarin) or toxins (e.g., cobratoxin) act as inhibitors or blockers of AChE. Blocking of the enzyme-stimulated nerve conduction leads to rapid paralysis of vital functions of living systems. Thus, the assembly described here may be considered as a biomaterial−semiconductor hybrid system for biosensors of biological warfare.

Recently, we reported on the organization of a CdS-NP/acetylcholine esterase (AChE) hybrid system on a Au-electrode and on the photoelectrochemical detection of the enzyme inhibitors.[20] In the reported system, the biocatalyzed hydrolysis of acetylthiocholine (**1**) generates in situ the thiocholine (**2**) that acts as an electron donor for the photocurrent generation in the system. In the presence of inhibitors, the biocatalyzed hydrolysis of **1** is inhibited, and the photocurrent generation is blocked. The fact that the Au−CdS nanoparticle array enables the SPR readout of the photoelectrochemical functions of the system suggests that the assembly of the AChE biocatalyst on the system would enable the SPR probing of the enzyme activity and its inhibition. Scheme 2 depicts the assembly of the AChE−Au−CdS nanoparticle hybrid system on the Au-coated glass slide and its operation under irradiation. The stepwise formation of the biocatalytic structure could be followed by SPR spectroscopy. Parallel microgravimetric quartz-crystal-microbalance analysis of the stepwise assembly of the array reveals that the surface coverage of AChE is ca. 3.9×10^{-2} mol·cm^{-2}. Figure 6 shows the SPR spectra upon illumination of the system at

Figure 6. The SPR spectra corresponding to the Au electrode surface modified with the Au-NP/CdS-NP/acetylcholine esterase (AChE) hybrid system upon illumination in the presence of various concentrations of acetylthiocholine (**1**): (a) 0 mM, (b) 6 mM, (c) 12 mM, (d) 30 mM. Inset: Calibration plot of the plasmon angle shifts at different acetylthiocholine concentrations.

different concentrations of acetylthiocholine (**1**). As the concentration of acetylthiocholine increases, the plasmon angles are shifted to higher values, and at concentrations of **1** that are higher than 1.5×10^{-2} M the changes in the plasmon angle reach saturation with a shift in the plasmon angle that is ca. $\Delta\theta = 0.35°$, Figure 6, inset. Control experiments reveal that addition of **1** to the system does not have any effect on the SPR spectrum of the assembly without the illumination. Also, irradiation of the Au−CdS nanoparticle array that lacks AChE in the presence of **1** does not alter the SPR spectra of the system. These results are consistent with the fact that the biocatalyzed hydrolysis of **1** yields thiocholine (**2**) that acts as an electron donor for the valence-band holes generated in CdS-NP upon irradiation of the system. The transport of conduction band electrons to the Au-nanoparticles with the concomitant oxidation of thiocholine (**2**) by the valence-band holes, results in the charging of the Au-particles and the respective changes in the SPR spectra.

The compound 1,5-bis(4-allyldimethylammoniumphenyl)-pentane-3-one dibromide (anticholinesterase BW284c51) (**3**), (see Scheme 2), is known to act as an inhibitor for AChE.[34] Thus, in the presence of **3** the AChE-biocatalyzed hydrolysis is inhibited, and this is expected to block the photoelectrochemical response of the AChE−Au−CdS array. This is expected to be reflected in the SPR spectra by shifting the plasmon angle of the system to lower values due to the blockage of the holes scavenging by the donor and hence due to the decreased charging of the Au-NP by the photoinduced electron transfer. Figure 7 shows the SPR spectra of the AChE−Au−CdS array upon irradiation in the presence of acetylthiocholine
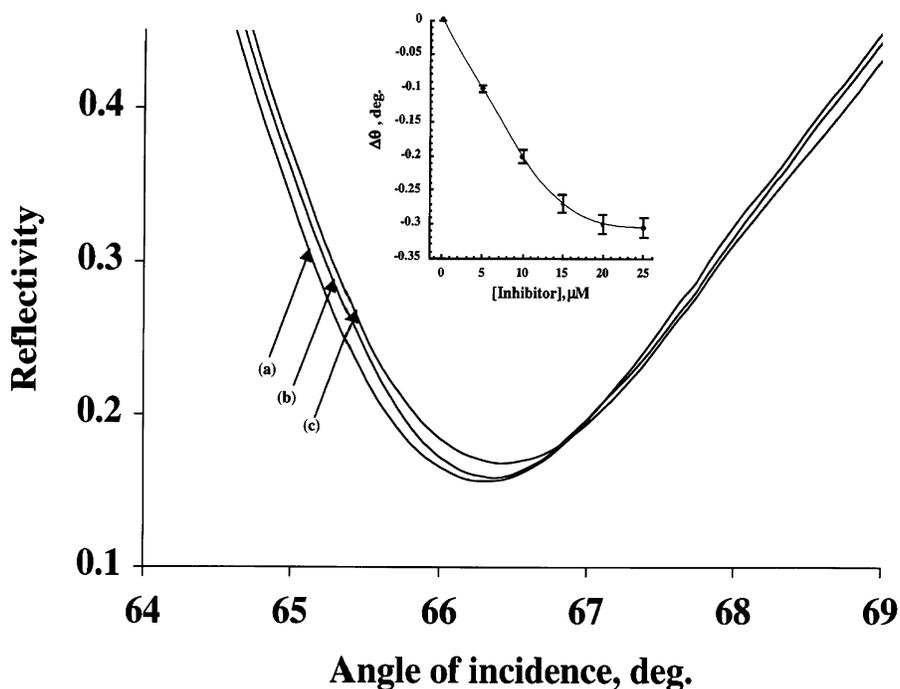
(**1**), 1.2×10^{-2} M, in the absence of **3**, curve (a), and upon the addition of different concentrations of the inhibitor **3**, curves (b) and (c). As the concentration of **3** is elevated, the plasmon angles are shifted to lower values, consistent with the inhibition of the enzyme and the blockage of the photoelectrochemical functions of this system. Figure 7, inset, shows the calibration curve that corresponds to the changes in the plasmon angles at different concentrations of the inhibitor **3**. The inhibitor can be detected with a sensitivity limit of 1×10^{-6} M. Thus, the minute perturbation of the photoinduced charging of the Au-NP in the presence of the inhibitor **3** are sufficient to affect the resulting SPR spectra.

Conclusions

The present study has demonstrated the analysis of the photoelectrochemical response of composite Au-NP and semiconductor nanoparticle arrays on gold surfaces by means of surface plasmon resonance (SPR) spectroscopy. We reveal that the cystamine layer on the electrode and the monolayer capping of the Au-nanoparticle form a barrier for electron transfer between the metal particle and the bulk SPR active surface. This barrier allows the photoelectrochemical charging of the Au-NP on the electrode. The resulting plasmon−plasmon coupling between the nanoparticle and the bulk Au surface changes the SPR spectrum of the system and enables the probing of the photoelectrochemical response of the system. Besides the fundamental interest in the observed phenomenon, it has significant practical implications. In the present report we demonstrate that a hybrid system consisting of AChE and Au-NP/CdS-NP array is an active structure for the SPR transduction of the enzyme activity and its inhibition. The fact that other enzymes may be coupled to the Au-semiconductor nanoparticle arrays and activate their photoelectrochemical functions suggests

(33) Bokris, J. O'M.; Reddy, A. K. N.; Gamboa-Aldeco, M. *Modern Electrochemistry*, 2nd ed.; Kluwer Academic: Dordrecht, The Netherlands, 2000; Vol. 2A.

(34) Barman, T. E. *Enzyme Handbook*; Springer-Verlag: New York, 1969; Vol. 2, pp 508−509.

Figure 7. The SPR spectra corresponding to the Au surface modified with the Au-NP/CdS-NP/acetylcholine esterase (AChE) hybrid system upon illumination in the presence of acetylthiocholine (**1**), 12 mM, and in the presence of variable concentrations of inhibitor **3**: (a) 0 mM, (b) 10 μM, (c) 20 μM. Inset: Calibration plot of the plasmon angle shifts at different concentrations of the added inhibitor **3**.

that the method could be further developed for other enzyme/ Au-semiconductor nanoparticle systems. Furthermore, recent research activities demonstrated that nucleic acid-functionalized semiconductor nanoparticles (e.g., CdS)[35] linked to electrodes by the cross-linked hybridization with a complementary DNA, yield, upon hybridization, photocurrents. The organization of

DNA-cross-linked Au-NP and semiconductor nanoparticles on bulk Au surfaces could provide a new approach to develop SPR DNA sensor systems based on the photoelectrochemical functions of the arrays.

(35) (a) Pathak, S.; Choi, S.-K.; Arnheim, N.; Thompson, M. E. *J. Am. Chem. Soc.* **2001**, *123*, 4103−4104. (b) Willner, I.; Patolsky, F.; Wasserman, J. *Angew. Chem., Int. Ed.* **2001**, *40*, 1861−1864.